Synthesis, X-ray Diffraction, Differential Scanning Calorimetry, and Magnetic Susceptibility Studies of a Series of Binuclear Ruthenium(II) Carboxylates Giving Liquid-Crystalline Phases

Laurence Bonnet, Fabio D. Cukiernik, Pascale Maldivi,*
Anne-Marie Giroud-Godquin, and Jean-Claude Marchon

CEA/Département de Recherche Fondamentale sur la Matière Condensée, CNRS/Laboratoire de Chimie de Coordination (URA 1194), SESAM/CC, Centre d'Etudes Nucléaires de Grenoble, BP 85 X, 38041 Grenoble, France

Mohammed Ibn-Elhaj, Daniel Guillon, and Antoine Skoulios

Groupe des Matériaux Organiques, Institut de Physique et Chimie des Matériaux de Strasbourg, UMR 46 CNRS-ULP-EHICS, 6, Rue Boussingault, 67083 Strasbourg Cedex, France

Received June 29, 1993. Revised Manuscript Received October 14, 1993®

A wide series of diruthenium(II,II) tetracarboxylates of general formula $Ru_2(RCOO)_4$ was prepared; the carboxylate substituents include linear alkyl chains (R = C_4H_9 to $C_{19}H_{39}$), unsaturated chains (R = $CH_2{=}CH(CH_2)_8{-}$, $(CH_3)_2C{=}CHCH_2CH_2CH(CH_3)CH_2{-}$) as well as a fluorinated chain (R = $C_7F_{15}{-}$). An adduct obtained by pyrazine intercalation was also characterized (R = $C_{11}H_{23}{-}$). The mesomorphic behavior of these compounds was investigated by differential scanning calorimetry and X-ray diffraction. A thermotropic columnar mesophase was observed above ca. 100 °C for all complexes except the perfluoro compound and the pyrazine adduct. Unsaturation in the peripheral alkyl chains strongly depresses the transition temperature to the liquid-crystalline phase. The magnetic susceptibility of three members of the series was measured in the range 6-400 K. A rigorous analytical expression of the magnetic susceptibility vs temperature was derived from the $(\pi^*)^2(\delta^*)^2$ electronic configuration for the ground state of a diruthenium(II,II) core, by applying a spin-orbit Hamiltonian, and the data were successfully analyzed on this basis.

Introduction

Binuclear complexes of carboxylic acids with transition metals such as Cu(II), Rh(II), Ru(II), and Mo(II) are known to exhibit the so-called "lantern" or "paddle-wheel" core exemplified by the structure of copper acetate dihydrate $Cu_2(CH_3COO)_4{\cdot}2H_2O$. In earlier work from our laboratories, we have fully characterized the liquid-crystalline properties of long-chain carboxylate complexes of Cu(II),[1] Rh(II),[2] and Ru(II),[3] using hot-stage polarizing optical microscopy, differential scanning calorimetry (DSC) and X-ray diffraction studies. Furthermore, we have taken advantage of the presence of metal atoms to gain additional information on the structural changes attending the crystal-to-mesophase transition using copper and rhodium K-edge EXAFS spectroscopy,[4] infrared (IR) and Raman spectroscopies,[5] and magnetic susceptibility measurements.[3,6]

The following structural features emerge from our studies of the Cu(II) and Rh(II) carboxylate mesogens. In both the crystalline and mesomorphic phases, the axial positions of the molecules are occupied by a carboxylate oxygen atom belonging to a neighboring complex,[4] leading to pseudopolymeric chains. In this respect, the solid-state structures of long-chain Cu(II) or Rh(II) carboxylates are similar to those of the short-chain analogues, copper and rhodium butyrates.[7] In the liquid-crystalline phase, the axes of these chains are located at the nodes of a two-dimensional hexagonal array.[1] The backbone of each column is made up of regularly stacked binuclear cores, and it is surrounded by "melted" aliphatic chains. Intermolecular cohesion is brought about by axial metal-oxygen coordination.

We were interested in extending these studies to the ruthenium(II) analogues for several reasons. First, these compounds offer us an opportunity to investigate further the influence of the metal center and of multiple metal-metal bonding[8] on mesomorphic behavior. This point has

® Abstract published in *Advance ACS Abstracts,* November 15, 1993.

(1) (a) Abied, H.; Guillon, D.; Skoulios, A.; Weber, P.; Giroud-Godquin, A. M.; Marchon, J. C. *Liq. Cryst.* **1987**, *2*, 269. (b) Ibn-Elhaj, M.; Guillon, D.; Skoulios, A.; Giroud-Godquin, A. M.; Maldivi, P. *Liq. Cryst.* **1992**, *11*, 731.

(2) Giroud-Godquin, A. M.; Marchon, J. C.; Guillon, D.; Skoulios, A. *J. Phys. Chem.* **1986**, *90*, 5502.

(3) Maldivi, P.; Giroud-Godquin, A. M.; Marchon, J. C.; Guillon, D.; Skoulios, A. *Chem. Phys. Lett.* **1989**, *157*, 552.

(4) (a) Abied, H.; Guillon, D.; Skoulios, A.; Dexpert, H.; Giroud-Godquin, A. M.; Marchon, J. C. *J. Phys., Paris.* **1988**, *49*, 345. (b) Maldivi, P.; Guillon, D.; Giroud-Godquin, A. M.; Marchon, J. C.; Abied, H.; Dexpert, H.; Skoulios, A. *J. Chim. Phys. Paris.* **1989**, *86*, 1651. (c) Ibn-Elhaj, M.; Guillon, D.; Skoulios, A.; Maldivi, P.; Giroud-Godquin, A. M.; Marchon, J. C. *J. Phys. 2 France.* **1992**, *2*, 2237.

(5) (a) Strommen, D. P.; Giroud-Godquin, A. M.; Maldivi, P.; Marchon, J. C.; Marchon, B. *Liq. Cryst.* **1987**, *2*, 689. (b) Poizat, O.; Strommen, D. P.; Maldivi, P.; Giroud-Godquin, A. M.; Marchon, J. C. *Inorg. Chem.* **1990**, *29*, 4851.

(6) Giroud-Godquin, A. M.; Latour, J. M.; Marchon, J. C. *Inorg. Chem.* **1985**, *24*, 4452.

(7) (a) Campbell, G. C.; Haw, J. F. *Inorg. Chem.* **1988**, *27*, 3706. (b) Cotton, F. A.; Shiu, K. B. *Rev. Chim. Miner.* **1986**, *23*, 14.

(8) Norman, J. G.; Renzoni, G. E.; Case, D. A. *J. Am. Chem. Soc.* **1979**, *101*, 5256.

0897-4756/94/2806-0031$04.50/0 © 1994 American Chemical Society

Scheme 1

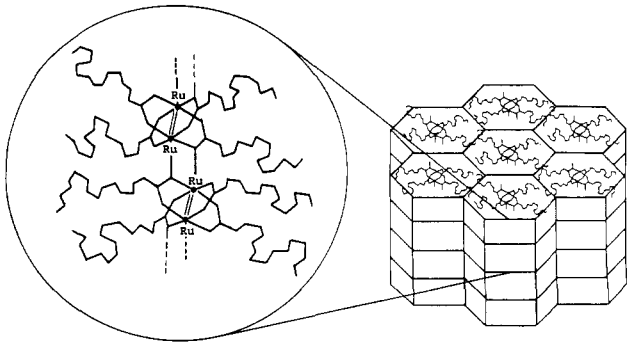

Table 1. Elemental Analysis Data (C, H, Ru)

	C, %		H, %		Ru, %	
compound	exp	calc	exp	calc	exp	calc
C5Ru	39.32	39.6	5.93	5.98	30.45	33.32
C7Ru	45.94	46.78	7.14	7.29	26.47	28.12
C8Ru	49.49	49.59	7.85	7.80	23.29	26.08
C10Ru	51.15	54.15	7.88	8.63	22.58	22.78
C11Ru	55.38	56.02	8.99	8.97	20.45	21.43
C12Ru	57.38	57.69	9.44	9.28	20.33	20.23
C14Ru	59.69	60.51	9.86	9.79	18.37	18.18
C16Ru	62.23	62.81	10.15	10.21	16.21	16.52
C18Ru	64.26	64.73	10.66	10.55	14.62	15.13
C20Ru	65.26	66.35	10.78	10.86	13.73	13.96
C10′Ru	54.27	54.65	7.80	7.79	23.14	22.99
C11′Ru	55.58	56.51	8.21	8.19	21.43	21.61
C8FRu[a]	24.58	24.00	1.03	0.80	10.56	10.10
C12RuPz[b]	56.54	57.86	8.84	8.96	18.48	18.73

[a] F %: exp 52.64, calc 57.00. [b] N %: exp 2.7, calc 2.57.

been alluded to in preliminary reports.[3,9] Second, these Ru(II) species deserve special interest due to their peculiar electronic properties, since they exhibit, in addition to their double metal–metal bond, a triplet group state.[3,8,10] These features combined with the unidimensional nature of the mesomorphic phase (see Scheme 1) could lead to materials with novel properties.

In view of undertaking a thorough study of their mesomorphic and electronic properties, we have synthesized a wide series of Ru(II) carboxylate complexes with linear, unsaturated, and fluorinated side chains. To increase the "communication" between the metallic cores, we have also investigated a compound obtained by intercalation of pyrazine. A report of our investigations by DSC, X-ray diffraction and magnetic susceptibility measurements is given below.

Experimental Section

Syntheses. The ruthenium(II,II) tetracarboxylates being air sensitive, specially in solution, all the syntheses were carried out under argon, in a glovebox. All solvents were of commercial grade and carefully degassed before use.

The experimental conditions (solvents, temperature, reaction time) have been optimized for each chain length, and they are detailed below for each compound.

The purity of all the compounds has been checked by elemental analyses, including the ruthenium element. All the results are reported in Table 1.

C2Ru:$Ru_2(CH_3COO)_4(H_2O)_2$. A solution of 1.4 g of $Ru_2(CH_3COO)_4Cl$ (2.96 mmol) in 800 mL of water was concentrated to 250 mL and then degassed. A deoxygenated aqueous solution of 0.75 M chromium(II) chloride (8 mL) was added slowly and a precipitate appeared. After this stirred for 15 min, the yellow-brown precipitate was filtered, and dried under vacuum; yield 56%.

C5Ru. A red solution of 0.250 g of C4Ru (0.45 mmol, synthesis described in ref 3) in 1.5 g of valeric acid (13 mmol) was heated under reflux for 10 min with constant stirring. The mixture was allowed to cool to room temperature, and a brown precipitate appeared, which was filtered and washed with *n*-heptane. The product was then dried under vacuum for 24 h; yield 85%.

C7Ru. The same procedure as described above was followed, starting with 0.250 g (0.45 mmol) of C4Ru and 1.5 g (10 mmol) of heptanoic acid; yield 75%.

C8Ru. The first step was similar to the procedure described for C7Ru, with 0.5 g of C4Ru (0.9 mmol) and 3 g of octanoic acid (19 mmol). After washing with heptane, the precipitate was dissolved in 3 mL of hot octanoic acid, and the compound which precipitated upon cooling was filtered and suspended in 10 mL of vigorously stirred heptane at room temperature for 24 h. The final compound was collected by suction filtration and dried under vacuum; yield 58%.

C10Ru. Decanoic acid (0.314 g, 1.8 mmol) was added to an aqueous solution of ruthenium acetate (0.200 g, 0.42 mmol in 300 mL). After 5 days of constant stirring at room temperature, the brown precipitate which was formed was extracted twice with 20 mL of heptane. The final product was isolated by concentration to dryness of the organic phase; yield 35%.

C11Ru. A solution of 0.5 g of C4Ru (0.9 mmol) and 3 g (16 mmol) of undecanoic acid in 30 mL of ethanol was kept under stirring at room temperature for 5 days. The brown precipitate which formed was filtered and recrystallized twice in 8 mL of hot ethanol; yield 51%.

C12Ru. A solution of 1.020 g of C4Ru (1.85 mmol) and 4.7 g (23.5 mmol) of dodecanoic acid (lauric acid) in 150 mL of ethanol was kept with constant stirring at room temperature for 15 days. The yellow-brown precipitate formed was collected by suction filtration and then recrystallized twice in 40 mL of hot ethanol; yield 63%.

C14Ru. The procedure was the same as described for C11Ru, with 0.25 g of C4Ru (0.45 mmol) and 1 g (2.2 mmol) of tetradecanoic acid (myristic acid); yield 38%.

C16Ru. A solution prepared with 0.25 g of C4Ru (0.45 mmol) and 1.02 g (4 mmol) of hexadecanoic acid (palmitic acid) in 60 mL of ethanol was kept at room temperature with constant stirring for 5 days. After filtration, the brown powder was recrystallized from 30 mL of hot heptane; yield 68%.

C18Ru. Octadecanoic acid (stearic acid, 1.14 g, 4.01 mmol) and 0.25 g of C4Ru (0.45 mmol) were dissolved in 110 mL ethanol. After stirring 5 days of room temperature, the brown precipitate was filtered and recrystallized in 5 mL of hot heptane; yield 55%.

C20Ru. Eicosanoic acid (1.440 g, 4.6 mmol) and 0.200 g of C4Ru (0.36 mmol) are dissolved in 60 mL of hot ethanol. After 10 min of refluxing with constant stirring, the mixture was cooled down to room temperature and a yellow-brown precipitate was formed. It was isolated by suction filtration and then recrystallized twice in 10 mL of hot ethanol; yield 50%.

C10′Ru. An emulsion was prepared with 0.388 g of citronellic acid (2.28 mmol) in 300 mL of water in which 0.250 g of C2Ru (0.57 mmol) was previously dissolved. After stirring 7 days at room temperature, the product was extracted twice with 20 mL of heptane. The resulting organic phase was concentrated to dryness; yield 55%.

C11′Ru. A mixture was prepared with 0.200 g of C2Ru (0.42 mmol) dissolved in 300 mL water and 0.340 g (1.8 mmol) of undecenoic acid dissolved in 2 mL of heptane. The resulting suspension was stirred for 7 days at room temperature, and the final complex was extracted with 20 mL of heptane and evaporated to dryness; yield 20%.

C8FRu. C4Ru (0.500 g, 0.9 mmol) and 1.5 g of perfluorooctanoic acid (3.6 mmol) were dissolved in 25 mL of ethanol. The solution was kept at room temperature with constant stirring for 5 days. It was then concentrated to dryness and recrystallized from a mixture of 1 mL of THF/4 mL of hexane. By cooling down to −20 °C, a red precipitate was formed which was isolated by suction filtration; yield 22%.

C12RuPz. Pyrazine (16 mg, 0.2 mmol) dissolved in 2 mL of ethanol were added to a hot ethanolic solution of C12Ru (0.200

(9) Cayton, R. H.; Chisholm, M. H.; Darrington, F. D. *Angew. Chem., Int. Ed. Engl.* **1990**, *29*, 1481.
(10) Cotton, F. A.; Matusz, M. *J. Am. Chem. Soc.* **1988**, *110*, 5761.

g, 0.2 mmol, in 10 mL). A dark purple precipitate appeared immediately. After cooling down to room temperature, the crude product was collected by suction filtration, washed with small amounts of ethanol, and then dried under vacuum; yield 78%.

Physical Measurements. Infrared spectra were recorded on a Beckman IR 4250 spectrometer. Samples were prepared as pressed pellets with KBr.

Thermodynamical parameters of the crystal-to-mesophase transition were measured on a Mettler FP 85 calorimeter. The samples were contained in aluminum pans sealed under argon, in a glovebox. The thermograms were recorded between 340 and 440 K, with a scanning rate of 5 °C/min, during several successive heating and cooling cycles.

For X-ray diffraction experiments, the powdered samples were contained in Lindemann capillaries (1-mm diameter). The patterns were recorded photographically using monochromatic Cu $K\alpha_1$ radiation and a Guinier focusing camera equipped with a bent quartz monochromator. The sample temperature was controlled to 0.1 °C, by an electrical oven.

The magnetic susceptibility measurements were performed on a Quantum Design MPMS SQUID susceptometer, in a magnetic field of 5000 G, between 6 and 400 K. The sample holder was a small plastic pan filled under argon with the powdered sample. The raw magnetic data were corrected from the diamagnetic contribution of the sample holder and from the diamagnetism of the ligands and the metal atoms. This diamagnetic contribution was evaluated by using Pascal's constants[11] and the calculated values for the four compounds studied are reported in Table 2. In the case of the C12Ru compound, the measurements have been carried out at three different magnetic fields: 5000, 15 000, and 25 000 G. The experimental values of the molar magnetic susceptibility were found to be independent of the magnetic field in that range.

Results and Discussion

Syntheses and Characterization of the Complexes. The general formula of binuclear ruthenium(II) carboxylates is $Ru_2(RCOO)_4$. For linear chain complexes, which will be noted as CnRu for the sake of simplicity, R is $CH_3(CH_2)_{n-2}-$. In this study, the total number of carbon atoms in a chain, n, was n = 5, 7, 8, 9, 10, 11, 12, 14, 16, 18, 20. Two unsaturated chain analogues have also been studied, with R = $CH_2{=}CH(CH_2)_8-$ (from undecylenic acid), noted as C11′Ru and R = $(CH_3)_2C{=}CHCH_2CH_2CH(CH_3)CH_2-$ (from citronellic acid) noted as C10′Ru.

The pyrazine adduct was obtained with the dodecanoate analogue, and the resulting product will be noted C12RuPz. Despite the absence of crystallographic structure on such species, we have some strong experimental evidence, as we will see later, that the resulting adduct has a polymeric structure similar to that of the copper acetate–pyrazine adduct:[12]

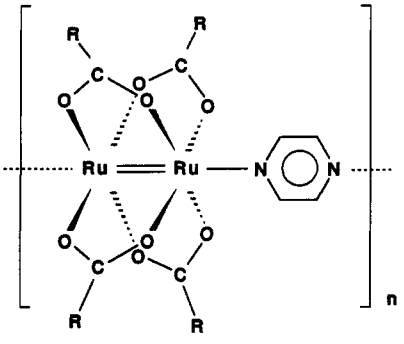

(11) Selwood, P. W. *Magnetochemistry*, 2nd ed.; Interscience: New York, 1956; Chapter V.

(12) Morosin, B.; Hughes, R. C.; Soos, Z. G. *Acta Crystallogr. B* **1975**, *31*, 762.

Table 2. Diamagnetic Susceptibilities of the CnRu Species from Pascal's Constants[11]

compound	X_{dia} (cm³/mol)
C10′Ru	-549.5×10^{-6}
C11′Ru	-551.5×10^{-6}
C12Ru	-644.4×10^{-6}
C12RuPz	-690.0×10^{-6}

Finally, one complex derived from a perfluorinated acid was investigated: ruthenium perfluorooctanoate, where R = $C_7F_{15}-$, which will be noted as C8FRu.

All these compounds have been characterized by infrared spectroscopy and elemental analyses.

Complexes of linear fatty acids with n = 5, 7, 8, 11, 12, 14, 16, 18, and 20, and of perfluorooctanoic acid were obtained using the same synthetic pathway as already described in a preliminary communication,[3] starting with ruthenium butyrate and substituting the four carboxylate ligands by the corresponding acid:

$$Ru_2(C_3H_7COO)_4 + 4RCOOH \rightarrow Ru_2(RCOO)_4 + 4C_3H_7COOH$$

The complexes C10Ru, C10′Ru, and C11′Ru were obtained by a similar procedure, but starting with ruthenium acetate $Ru_2(CH_3COO)_4(H_2O)_2$ instead of the butyrate. Ruthenium acetate was synthesized in the same way as ruthenium butyrate,[3] by reduction of an aqueous solution of chlorotetraacetatodiruthenium(II,III), $Ru_2(CH_3COO)_4Cl$, by chromium(II) chloride. The pyrazine complex was readily obtained by adding a stoichiometric amount of pyrazine to an ethanol solution of C12Ru. Experimental procedures as well as characterization by elemental analysis of all complexes are described in the experimental section.

Infrared spectroscopy has proved informative, especially in the region between 1400 and 1700 cm^{-1} where the symmetrical and asymmetrical stretching modes of the carbonyl groups appear. The corresponding frequencies as well as their difference, are highly correlated to the nature of the metal atoms and of the carboxylato ligand, and they are also influenced by the coordination mode of the carboxylate. The main features of the infrared spectra of linear or unsaturated chain analogues, as well as of the perfluorinated complex and the pyrazine adduct, are reported in Table 3.

The ν_s(CO) and ν_{as}(CO) frequencies found for CnRu, C10′Ru, and C11′Ru are respectively ca. 1440 and 1550 cm^{-1}, irrespective of the chain length. These values are in good agreement with those (1432 and 1556 cm^{-1}, respectively) published for the propionate analogue.[13] In the case of long-chain derivatives, the main additional feature was the presence of several strong bands between 2800 and 3000 cm^{-1}, corresponding to CH_2 and CH_3 stretching modes. Also present is a strong band at 1470 cm^{-1}, corresponding to the CH_2 bending mode. For one of the unsaturated analogues, C11′Ru, the stretching mode of the terminal double bond was visible as a medium-weak band at 1635 cm^{-1}.

The frequencies corresponding to the ν_s(CO) and ν_{as}(CO) modes of the perfluorinated compound C8FRu were found respectively at 1460 and 1660 cm^{-1}. This is in good agreement with the published values found for ruthenium

(13) Lindsay, A. J.; Wilkinson, G.; Motevalli, M.; Hursthouse, M. B. *J. Chem. Soc., Dalton Trans.* **1985**, 2321.

Table 3. Selected Infrared Absorption Bands (cm^{-1}) of Ruthenium(II) Carboxylates

compound	ν_{as}(CO)	ν_s(CO)	others
CnRu (n = 5, 7, 8, 9, 10, 11, 12, 14, 16, 18, 20)	1550	1435	CH_2, CH_3: 2850, 2870, 2920, 2955, 1470
C10′Ru	1545	1430	
C11′Ru	1545	1430	C=C: 1635
C8FRu	1660	1460	CF_2, CF_3: 1230
			1245
			1270
C12RuPz	1560	1430	CH_{arom}: 3090

trifluoroacetate.[14] The CH_2 stretching modes of axially coordinated THF molecules appear between 2800 and 3000 cm^{-1}. The CF_2 and CF_3 stretching modes are visible as several intense bands between 1200 and 1300 cm^{-1}.

Finally, infrared spectroscopy was useful in establishing the structure of the pyrazine adduct. This adduct appears as a very dark purple powder, whereas the starting ruthenium carboxylate C12Ru is a yellow-brown powder. This striking difference could be assigned to a possible decomposition of the tetracarboxylate core upon reaction with pyrazine. However, the infrared spectrum of C12RuPz was found to exhibit all the characteristic features of the C12Ru complex itself. Noteworthy were the ν_s(CO) and ν_{as}(CO) bands respectively at 1430 and 1560 cm^{-1}. In addition, the presence of pyrazine could be confirmed by the appearance of several characteristic bands in the fingerprint region, as well as above 3000 cm^{-1}, where the weak CH (aromatic) stretching band appeared at 3090 cm^{-1}. However, the bands corresponding to the aromatic rings (ca. 1520 and 1580 cm^{-1}) were not detected, whereas the resonance Raman spectrum of this species clearly exhibited these bands.[15] This observation led us to assume a bridging coordination mode, in which the aromatic ring modes are not infrared active.[16] These spectral considerations, together with the observation of the complete insolubility of C12RuPz in all common solvents, led us to the safe conclusion that the C12RuPz complex is polymeric, with bridging pyrazine molecules, as described for the copper acetate analogue.[12]

Liquid-Crystalline Behavior. The ruthenium(II,II) tetracarboxylates are thermally unstable under oxygen, making difficult their observation with a polarizing optical microscope, even under a flow of argon. Thus the detection of their mesophases was carried out by DSC.

No liquid-crystalline phase could be detected for the perfluoro compound C8FRu or for the C12RuPz adduct. In the case of the fluorinated derivative, this absence of mesomorphism is most likely due to the high rigidity of the perfluorinated chains. On the other hand, pyrazine intercalation generates free space between alkyl-substituted cores which is detrimental to the formation of a compact columnar structure with parallel chains of molecules. This interpretation is corroborated by the results of Attard et al.[17] on some copper analogues and their complexes with pyrazine: no mesomorphic properties could be found for the adduct made with linear chain copper carboxylates. In contrast, the pyrazine complex with a branched chain carboxylate (dioctyl acetate) seemed to undergo a thermal transition to a mesophase. This mesomorphic behavior was assumed to be related to the presence of a bulky carboxylate which can fill the space more efficiently around the bridging pyrazine molecules. However, the X-ray diffraction patterns were somewhat different from those expected for a columnar hexagonal structure.

Table 4. Temperatures (°C) and Enthalpies (kJ mol^{-1}) of the Crystal-to-Mesophase Transition for $Ru_2(RCOO)_4$ As Measured by DSC

compound	T (°C)	ΔH (kJ mol^{-1})
C5Ru	158	20
C7Ru	113	54
C8Ru	103	48
C9Ru	96	40
C10Ru	98	76
C11Ru	97	78
C12Ru	99	66
C14Ru	98	66
C16Ru	102	149
C18Ru	98	145
C20Ru	104	155
C10′Ru	52.7	32.0
C11′Ru	79.2	54.0

We have observed a phase transition for all the linear and unsaturated chain species, and the thermodynamic data of the transition crystal → mesophase are reported in Table 4. The clearing temperature could not be reached for any of the compounds, due to sample decomposition.

The dependence of the transition temperature with the number of carbon atoms in the alkanoate is the same as that already observed for copper[1b] and rhodium[2] carboxylates, with two regimes: a decrease of the transition temperatures with increasing chain length for the short chain analogues than a leveling around 100 °C for the long-chain complexes. This leveling occurred around 100 °C for rhodium carboxylates, whereas it was found slightly higher (about 120 °C) for copper carboxylates. The higher stability of the crystalline phase of very long-chain copper carboxylates, compared to the second-row metal carboxylates, suggests better intermolecular cohesion in the crystalline phase of the copper complexes.

This dual regime seems independent of the metal and mainly governed by the aliphatic chains. Such a result corroborates our interpretation of the dependence of the crystal-to-mesophase transition temperatures with the number of carbon atoms.[1b] With short alkyl chains, the stability of the crystal is mainly governed by the cohesion of the metallic cores, and this structure is perturbed when the alkyl chains get longer. This situation leads to a decrease of the transition temperature for increasing n. For the long alkyl chain complexes, the stability of the crystal is dominated by the packing of the paraffinic chains, and it is favored when the chain length increases, until a limit where the crystal cohesion is almost entirely due to the paraffinic chain interactions. Above that limit, increasing the chain length does not influence the stability of the structure anymore.

An increase of the enthalpy with the number of carbon atoms is observed (see Table 4), although the dependence

(14) Lindsay, A. J.; Wilkinson, G.; Motevalli, M.; Hursthouse, M. B. *J. Chem. Soc., Dalton Trans.* **1987**, 2723.
(15) Cukiernik, F. D.; Poizat, O.; Maldivi, P.; Marchon, J. C. Work under progress.
(16) Metz, J.; Schneider, O.; Hanack, M. *Spectrochim. Acta* **1982**, *38A*, 1265.
(17) Attard, G. S.; Cullum, P. R. *Liq. Cryst.* **1990**, *8*, 299.

Table 5. Interlamellar Distances *d* (Å) in the Crystalline Phase for the C*n*Ru Compounds and for the Corresponding C*n*Cu Complexes, as a Function of *n* (Number of Carbon Atoms in the Carboxylate Chain)

	d (Å)	
n	Ru	Cu
7	19.2	18.7[b]
9	24.5[a]	24.5[b]
10	26.6	27.4[c]
12	31.7[a]	32.5[b]
14	35.4	36.3[b]
16	42.3	41.8[b]

[a] Taken from ref 3. [b] Taken from ref 1. [c] Calculated from ref 18.

deviates strongly from linearity. Linear behavior was observed for the Cu analogues.[1b] Numerous samples from different batches have been submitted to several heating–cooling processes, and the results were found to be reproducible. We assume that the fusion from the crystal to the mesophase possibly could be a more complex process than that followed by the copper analogues. This hypothesis finds support in the observation, in the thermograms of several ruthenium(II) carboxylates, of two components in the endothermic peak, which however could not be fully resolved.

X-ray diffraction measurements have been performed on powdered samples of C7Ru, C10Ru, C14Ru, and C16Ru at room temperature, for the crystalline phase, and at 120 °C for the mesophase.

The only crystallographic structures that were reported in the literature for ruthenium(II) carboxylates dealt with ruthenium(II) acetate axially coordinated by various solvents or complexing agents.[13,14] Thus we have assumed that the long-chain derivatives would exhibit similar structures to those observed for the Cu(II) analogues, which were found to be lamellar.[18] As shown below, this assumption has found strong support in the powder X-ray patterns of the higher homologues of Ru(II) carboxylates.

The X-ray patterns recorded at room temperature for the linear chain compounds contain a series of sharp equidistant Bragg reflections in the low-angle region, indicative of a lamellar structure. The values found for the lamellar spacings are reported in Table 5. They are very similar to those found for the copper analogues, supporting our assumption that the crystalline phases of ruthenium and copper long-chain carboxylates are isostructural.

The interlamellar spacing increases linearly with *n*, the number of carbon atoms, as shown on Figure 1. A least-squares linear fit led to

$$d(\text{Å}) = 1.81 + 2.48n \qquad \text{(A)}$$

The structure of the C10Cu analogue[18] is made up of sheets containing the bimetallic cores of the molecules, which are separated by two layers of extended aliphatic chains. The chain direction is tilted by about 18° with respect to the perpendicular of the layers. In the case of the CnRu species, the slope of the straight line (2.48 Å), as calculated above, gives the contribution of two C–C bonds to the lamellar spacing, and this value is lower than the distance of a zigzag of carbon atoms in a fully extended paraffin, which is 2.54 Å. The tilt angle was therefore calculated to be 12°, which is in reasonable agreement with the value obtained for the CnCu derivatives (18°),[1b] considering the limited accuracy of our experimental data.

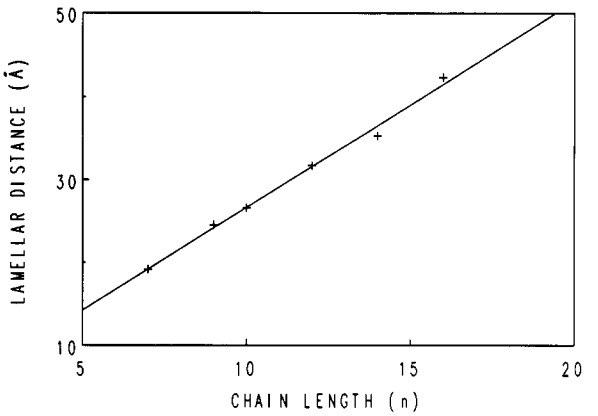

Figure 1. Interlamellar distances *d* (Å) in the crystalline phase as a function of the number of carbon atoms in the carboxylate. The straight line is the result of a linear regression as described in the text.

Table 6. Intercolumnar Distance *D* (Å) for the C*n*Ru Compounds and for the Corresponding C*n*Cu Complexes as a Function of *n* (Number of Carbon Atoms in the Carboxylate Chain)

	D (Å)	
n	Ru	Cu
9	17.6[a]	17.3[b]
10	18.2	
12	19.4[a]	19.9[b]
14	22.0	20.9[b]

[a] Taken from ref 3. [b] Taken from ref 1.

In the low-angle region of the X-ray patterns recorded at high temperature, several reflections with reciprocal spacings of $1:3^{1/2}:4^{1/2}:7^{1/2}:9^{1/2}$ are indicative of an hexagonal columnar mesophase. The quality of the patterns obtained for the C7Ru and C16Ru was not sufficient to extract the intercolumnar distance *D*. The values obtained for the C10Ru and C14Ru complexes are reported in Table 6 together with those already published for the C9Ru and C12Ru, and with the corresponding values of the copper species, when available. It appears clearly that the intercolumnar distance is somewhat independent of the nature of the metal atoms of the mesogen.

The X-ray patterns also show the presence of a packing order within the columns, with a repeating distance of 4.6 Å. This is quite similar to the results already reported for the copper analogues and for C9Ru and C12Ru.

Thus the same columnar hexagonal ordered mesophase was obtained throughout the series of copper and ruthenium carboxylates, and its structural parameters were found to vary mainly with the chain length.

Magnetic Properties. We have examined the magnetic behavior of four complexes: C12Ru, C10′Ru, C11′Ru, and C12RuPz by measurements of the magnetic susceptibility as a function of the temperature, between 6 and 400 K. The three Ru(II) carboxylates were found to exhibit very similar behavior to that previously described for similar complexes.[3,19] We show as an example on Figure 2 the molar magnetic susceptibility and the χT product of the compound C11′Ru as a function of temperature. The values of χT at room temperature (1.11 cm^3 K mol^{-1} for C12Ru, 1.24 cm^3 K mol^{-1} for C10′Ru, and 1.08 cm^3 K mol^{-1} for C11′Ru) are consistent with a triplet state ($S = 1$), as already observed for short-chain homologues[14,19] and

(18) Lomer, T. R.; Perera, K. *Acta Crystallogr. B* **1974**, *30*, 2912.

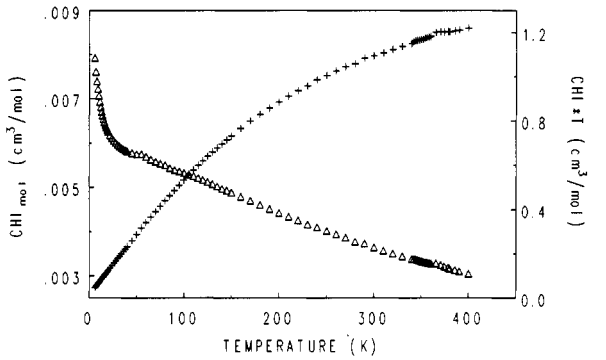

Figure 2. Experimental molar susceptibility χ (triangles) and χT product (crosses) as a function of temperature, for the C10′Ru complex.

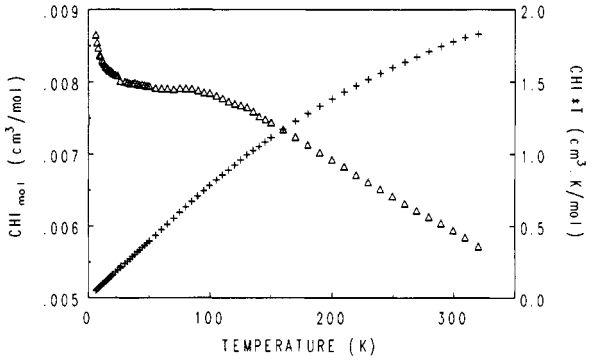

Figure 3. Experimental molar susceptibility χ (triangles) and χT product (crosses) as a function of temperature, for the C12RuPz complex.

predicted by Norman et al.,[8] on the basis of Xα calculations. The overall shape of the χ vs T curve is indicative of a strong deviation from a normal paramagnetic $S = 1$ system. It has been interpreted as arising from a strong zero-field splitting.[3,19] The recently investigated 2-hydroxypyridinate complexes of Ru(II),[20] which are isostructural and isoelectronic with the Ru(II) carboxylate species, exhibit a very similar magnetic behavior.

The molar magnetic susceptibility χ and the χT product versus temperature, for the C12RuPz complex, are represented on Figure 3. Examination of these curves indicates a magnetic behavior very similar to that described above for the Ru(II) carboxylates.

Another observation which could be made on the experimental results was the presence, for all three CnRu compounds, of a discontinuity in the magnetic susceptibility curve at a temperature identical to the transition temperature to the columnar mesophase (see Figure 1 in ref 3). This break is presumably due to some slight modification of the electronic structure, which attends the structural reorganization due to the melting process.

To be valid, an interpretation of the magnetic susceptibility data should be based on a thorough examination of the electronic structure of the Ru(II) carboxylates. The correct assignment of the exact electronic configuration of the highest occupied molecular orbital (HOMO) has been a challenge for a few years. The first theoretical Xα SW calculation was performed by Norman et al.[8] on $Ru_2(HCOO)_4$, and it predicted a double Ru–Ru bond, the HOMO being a nearly degenerate set of π^* and δ^*, occupied by four electrons. The ground state obtained was $(\pi^*)^3(\delta^*)^1$, and the first excited state $(\pi^*)^2(\delta^*)^2$ was separated by 2 kcal/mol from this ground state. This could account for the observed room-temperature magnetic moment, indicative of two unpaired electrons. To elucidate the problem of the actual ground-state population of the (π^*,δ^*) orbitals, a calculation of the magnetic susceptibility obtained with the $(\pi^*)^3(\delta^*)^1$ configuration was performed by Cotton et al.[20] This configuration gave rise to a ^3E ground state, which therefore was subject to a first order spin–orbit coupling: the resulting magnetic susceptibility thus calculated as a function of temperature could not account for the experimental data measured for the hydroxypyridinate complex. This calculation also showed that the only ground-state configuration consistent with the magnetic behavior of the Ru(II) hydroxypyridinate was $(\pi^*)^2(\delta^*)^2$, undergoing a zero-field splitting (ZFS). It is therefore reasonable to assume that the Ru(II) carboxylates will exhibit the same ground-state configuration.

As a matter of fact, the ZFS phenomenon is usually known for mononuclear species, and it is generally simply described with the spin Hamiltonian $\mathbf{H} = D(\mathbf{S}_z^2 - {}^1/_3\mathbf{S}(\mathbf{S} + 1))$. Now the species that are discussed here are more complex as they are binuclear and possess a double metal–metal bond. The question therefore arises as to the validity of using directly this spin Hamiltonian to treat the magnetic behavior of such binuclear systems.

Within that frame, we have performed a complete calculation of the expected magnetic susceptibility arising from a $(\pi^*)^2(\delta^*)^2$ ground-state configuration undergoing a zero-field splitting. The physical meaning of that phenomenon is the existence of an orbital anisotropy, due to some crystal-field distortion, which is transmitted to the electronic spin via the spin–orbit coupling, thus leading to a magnetic anisotropy.[21,22] In the case of the Ru(II) carboxylates, this anisotropy was assumed to be axial, and the symmetry of the bimetallic core was assumed to be D_{4h}.

This physical interpretation is generally described by the second-order spin–orbit coupling which, when applied to the ground state, "mixes" that state with another orbitally degenerate triplet excited state, which lies at an energy δ above the ground state.[22] In the case of the Ru(II) carboxylates, the ground-state ^3A is derived from the $(\pi^*)^2(\delta^*)^2$ configuration, and an obvious ^3E excited-state arises from the $(\pi^*)^3(\delta^*)^1$ configuration. The complete calculation, which will be published elsewhere[23] leads to the following expressions for the molar magnetic susceptibility:

$$\chi_{\parallel} = Ng_{\parallel}^2\beta^2/kT \cdot 2e^{-D/kT}/(1 + 2e^{-D/kT})$$

$$\chi_{\perp} = Ng_{\perp}^2\beta^2/kT \cdot 2kT/D \cdot (1 - e^{-D/kT})/(1 + 2e^{-D/kT})$$

It is important to note that these expressions are identical to those of the magnetic susceptibility of a triplet state undergoing a ZFS calculated by means of the usual spin Hamiltonian. Thus the phenomenological approach based

(19) (a) Cotton, F. A.; Miskowski, V. M.; Zhong, B. *J. Am. Chem. Soc.* **1989**, *111*, 6177. (b) Cotton, F. A.; Kim, Y.; Ren, T. *Polyhedron* **1993**, *12*, 607.

(20) Cotton, F. A.; Ren, T.; Eglin, J. L. *Inorg. Chem.* **1991**, *30*, 2552.

(21) (a) O'Connor, C. J. *Prog. Inorg. Chem.* **1982**, *29*, 203. (b) Telser, J.; Miskowski, V. M.; Drago, R. S.; Wong, N. M. *Inorg. Chem.* **1985**, *24*, 4765.

(22) Carrington, A. *Microwave spectroscopy of free radicals*; Academic Press: New York, 1974; Chapter 10.

on ZFS that was used in previous papers[3,19] for the analysis of magnetic susceptibility data on Ru(II) carboxylates appears fully justified *a posteriori*.

The above calculation sheds some light on the physical origin of the magnetic behavior found for the Ru(II) carboxylates. Nevertheless, one question arises, as to the validity of the use of the second-order perturbation theory in such a system: to answer this question, we have to compare D to δ. We have a reasonable idea of the magnitude of the ZFS constant D, from the adjustments of experimental magnetic susceptibility curves vs temperature:[3,19] $D \approx 250$ cm^{-1}. The energy gap δ between the ^{3}A and ^{3}E states has been evaluated by means of a theoretical calculation on the $Ru_2(CH_3COO)_4$ moiety, with a local density method,[23] and it was found to be $\delta \approx 3000$ cm^{-1}. Under such conditions, the second-order perturbation method is therefore quite valid.

On the basis of this model, we have performed refinements of all the experimental results, for the crystalline phase only (6–320 K temperature range), with the susceptibility expression found above. In a second step, we have checked the possibility of interdimer exchange due to pyrazine intercalation. Thus we have carried out a second type of adjustment, by considering a contribution due to a weak intermolecular interaction in addition to the ZFS term. As the experimental data have been found to be independent of the magnetic field (see Experimental Section), our calculations were based on one set of experimental values of the magnetic susceptibility (at 5000 G) for each compound.

(*i*) *S = 1 with ZFS.* The experimental values of the molar magnetic susceptibility, for the four complexes, were first refined by the mathematical law $\chi(T)$ determined above. The magnetic measurements were carried out on powdered samples, thus the theoretical expression that we used in our refinements was the average $\chi_{ZFS} = {}^1/_3(\chi_\parallel + 2\chi_\perp)$, to which was added the temperature-independent paramagnetism (TIP) and a contribution due to a possible paramagnetic impurity within the sample. As a matter of fact, in the low-temperature region of the $\chi(T)$ curve (Figure 2), we observe an increase of the susceptibility with decreasing temperatures, whereas the susceptibility of a $S = 1$ + ZFS magnetic system should tend to a constant. This contribution, due to an impurity, was assumed to follow a simple Curie law. Therefore the complete equation of as a function of the temperature, which was used in our refinements was

$$\chi = (1 - \epsilon)(\chi_{ZFS} + \mathrm{TIP}) + \epsilon N\beta^2 g_i^2 S_i(S_i + 1)/kT \quad \text{(B)}$$

where χ_{ZFS} is the theoretical expression of the zero-field splitting term (as described above), ϵ is the percentage of the paramagnetic impurity, S_i and g_i being respectively the spin and the Lande factor of this impurity.

The refinements were achieved by a least-squares fitting procedure, with six adjustable parameters: D, $g_\parallel$, and $g_\perp$, ϵ, TIP, and g_i. The spin of the impurity was supposed to be $^1/_2$.

A very good agreement between experimental and calculated values was found for the four complexes studied. The values of the magnetic parameters, obtained for the best fits are reported in Table 7. The quality of fit was given by the factor $\sigma = (\sum(\chi_{exp} - \chi_{theo})^2)^{1/2}/(\sum\chi_{exp}^2)^{1/2}$ and was also reported in Table 7. An example of the good agreement between experimental and calculated values is illustrated on Figure 4 for C12Ru, which shows both experimental points and the theoretical curve calculated with the parameters reported in Table 7.

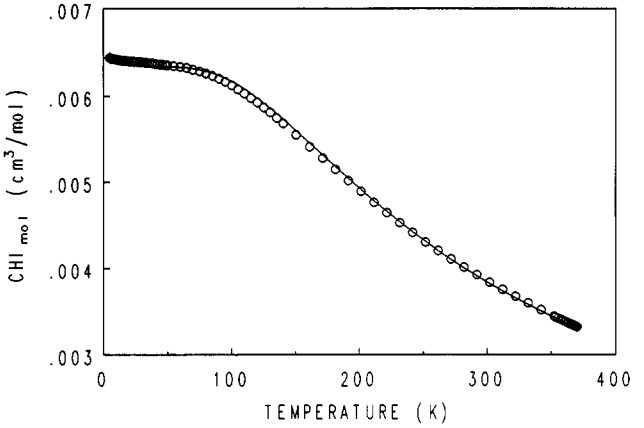

Figure 4. Experimental (open circles) and calculated (full line) curves of molar magnetic susceptibility as a function of temperature for the C12Ru complex. The calculated values were obtained with the magnetic parameters listed in Table 5.

Table 7. Magnetic Parameters: D (cm^{-1}), $g_\parallel$, $g_\perp$, TIP, ϵ (% Impurity), and σ (Goodness of Fit) Obtained for Least-Squares Adjustments of Magnetic Susceptibility Data

compound	D (cm^{-1})	$g_\parallel$	$g_\perp$	TIP	ϵ (%)	σ (×10^2)
C10′Ru	283	1.93	2.22	7×10^{-4}	4.3	2.2
C11′Ru	314	1.90	2.13	5×10^{-4}	3.5	1.7
C12Ru	270	1.92	2.11	6×10^{-4}	0.3	0.5
C12RuPz	291	2.07	2.13	2.3×10^{-3}	1.0	0.47

(*ii*) *S = 1 with ZFS and Weak Intermolecular Exchange.* In a second set of refinements, we have added in the theoretical expression $\chi(T)$ a contribution due to an intermolecular interaction. In the hypothesis of a weak exchange, we have used the molecular field approximation, which gives the expression of the magnetic susceptibility χ' of a molecular moiety interacting weakly with its neighbors:[21]

$$\chi' = \chi_{mol}/(1 - (2zJ/Ng^2\beta^2)\chi_{mol})$$

where χ_{mol} is the magnetic susceptibility of the isolated molecule, z the number of neighbors, and J the magnitude of the intermolecular interaction. This equation is valid when the magnitude of the exchange (measured by J) is much lower (5–10 times) than other types of intramolecular interactions.[21]

We have used this expression to adjust all the experimental data, where χ_{mol} was taken as

$$\chi_{mol} = \chi_{ZFS} + \mathrm{TIP}$$

and the total expression of the magnetic susceptibility was

$$\chi = (1 - \epsilon)\chi' + \epsilon N g_i^2 \beta^2 S_i(S_i + 1)/kT$$

to add the contribution of the impurity, as already described above. The procedure for the fits was essentially the same, with the following adjustable parameters: D, $g_\parallel$, and $g_\perp$, TIP, zJ, ϵ and g_i. We have tried several refinement processes, either by letting all parameters free or by fixing some of them (ϵ, g_i, D, ...) to the values obtained above, to decrease the number of floating parameters. Whatever the method, the calculations always led to the same result for all the compounds: no improvement of the refinements

(23) Grand, A.; Maldivi, P.; Subra, R. Unpublished work.

could be gained by the introduction of a supplementary parameter. Equivalent fits were obtained with various sets of magnetic parameters with either positive, null or negative values of zJ.

Thus, it seems difficult to draw an unambiguous conclusion about a hypothetical intermolecular exchange, even in the case of the pyrazine adduct. The latter compound can be compared to the isostructural mixed-valent ruthenium(II,III) carboxylates adducts with pyrazine (or phenazine) for which a weak intermolecular antiferromagnetic coupling has been observed.[24] A possible reason why no intermolecular interaction can be detected in the present system could come from the nature of the ground state. At low temperatures, where a possible weak intermolecular coupling could be detected, the only populated level is $S_z = 0$, due to the strong ZFS. If an anisotropic coupling is present, it will have no effect, acting on a $S_z = 0$ level. If this interaction is isotropic, it would be effective only on $\chi_\perp$, and to measure it, it would become necessary to get anisotropic measurements of the magnetic susceptibility, carried out on a single crystal.

Conclusion

We have presented in this paper a detailed investigation of the structural and electronic properties of a homologous series of binuclear Ru(II) carboxylates.

Close structural similarities have been found between the ruthenium and copper analogues, suggesting possible correlations between the molecular structure and the mesomorphic properties in this series of binuclear carboxylates, even if little crystallographic information is available for the ruthenium derivatives.

The influence of the transition metal is mainly apparent in the strong interaction which it creates between adjacent molecules, via the axial coordination by a neighboring oxygen atom. The aliphatic chains play an important role because they are responsible for the existence of a mesomorphic state and because the thermodynamic properties are related to the balance between the interactions of the paraffinic parts on one side and the cohesion of the polar metallic cores on the other.

The liquid-crystalline state is thus mainly due to the capability of the aliphatic chains to disorder when increasing the temperature, to reach a liquidlike state without destroying the intermolecular axial interactions between the polar cores which maintain the rigid backbone of the columns.

In the course of our studies on their magnetic behavior, it became necessary for us to perform a rigorous investigation of their electronic structure. Our calculations have led us to a complete description of the electronic ground state of the Ru(II)–Ru(II) bond within these species. This problem was not trivial due to the presence of a double bond between second-row transition metals. In parallel to this study, a theoretical investigation of their electronic configuration is under way, to clarify the difference between the results obtained by Norman et al.[8] which claimed a $(\pi^*)^3(\delta^*)^1$ ground state configuration and the actual one, proved to be $(\pi^*)^2(\delta^*)^2$.

In spite of the close proximity of the metallic centers and of the unidimensional character of the structure, no long-range magnetic interactions could be detected in these systems. In the absence of useful magnetic properties, these materials may reveal potential properties such as electronic conductivity or optical birefringence.[25]

Acknowledgment. We wish to thank Pr. Robert Subra (Université Joseph Fourier, Grenoble) and Dr. André Grand (UJF, Grenoble) for fruitful discussions, and Jean-François Jacquot for assistance with the magnetic susceptibility measurements.

(24) (a) Cotton, F. A.; Kim, Y.; Ren, T. *Inorg. Chem.* **1992**, *31*, 2723. (b) Cukiernik, F. D.; Giroud-Godquin, A. M.; Maldivi, P.; Marchon, J. C. *Inorg. Chim. Acta.* In press.

(25) (a) Bertram, C.; Bruce, D. W.; Dunmur, D. A.; Hunt, S. E.; Maitlis, P.; McCann, M. *J. Chem. Soc., Chem. Commun.* **1991**, 69. (b) Bruce, D. W.; Dunmur, D. A.; Maitlis, P.; Manterfield, M. M.; Orr, R. *J. Mater. Chem.* **1991**, *1*, 255.